THE ARGON MELTING CURVE TO VERY HIGH PRESSURES

C-S. Zha and R. Boehler
Department of Chemistry and Biochemistry
University of California
Los Angeles, CA 90024

and

D. A. Young and M. Ross
Lawrence Livermore National Laboratory
University of California
Livermore, CA 94550

Lawrence
Livermore
National
Laboratory

DISCLAIMER

THE ARGON MELTING CURVE TO VERY HIGH PRESSURES

C-S. Zha and R. Boehler

Department of Chemistry and Biochemistry

University of California

Los Angeles, California 90024

and

D. A. Young and M. Ross

Lawrence Livermore National Laboratory

University of California

Livermore, California 94550

ABSTRACT

The melting curve of Ar has been measured to 717 K and 60 kbar using a new interferometric technique in a diamond anvil cell. Theoretical calculations are in excellent agreement with the measurements.

I. INTRODUCTION

The properties of Ar at extreme conditions have been the subject of several recent investigations. In the preceding paper[1], the results of static diamond anvil studies in the solid were presented which extended the pressure range to 800 kbar, a large increase over earlier measurements[2]. Shockwave studies on the liquid which achieved pressures up to 900 kbar have now been supplemented by shock temperature measurements[3,4]. All of these data can be calculated with presently available statistical mechanical theories using a single intermolecular potential[1].

In contrast to these recent advances, no new measurements of the Ar melting curve have appeared since 1974[5]. In this piston-cylinder work the highest melting point obtained was 18 kbar at 360 K[6]. Although Grace and Kennedy reported melting data in 1967 to 26 kbar[7], these were not consistent with the other measurements made during that period and are often disregarded[8].

In this paper we present new experimental measurements of the Ar melting curve to 717 K and 60 kbar. These measurements greatly extend

the investigated pressure range and provide us with an excellent opportunity to test several different theories of melting. We find that the melting curve calculated using the intermolecular potential determined from the shock and static data is in excellent agreement with these new measurements.

II. EXPERIMENTAL

An externally heated diamond cell was used. Temperatures were measured with a calibrated thermocouple attached to the diamond, and pressures were obtained from the known pressure and temperature shifts of the ruby fluorescence line. The temperature dependent broadening of this line limits the range of this technique to about 700 K[9]. The gasketed diamond cell was loaded with liquid Ar, pressurized to over 20 kbar, and the cell was then slowly heated while monitoring pressure and temperature. At pressures below about 36 kbar, the melting of Ar was observed by the disappearance of the crystal grain boundaries of the solid. The temperature range of this process is about 10 degrees. Melting pressures and temperatures were taken when the Ar crystals were in equilibrium with the liquid.

Above about 36 kbar the grain boundaries between Ar crystals were no longer visible and melting was measured by monitoring an interference pattern produced between the diamonds using transmitted white light. When the temperature is changed, the interference pattern shifts continuously with respect to the wavelength due to a change in the refractive index of Ar. A strong discontinuous shift of the interference pattern is observed during melting, either by plotting the shift of one or more interference peaks versus temperature, or by recording the intensity of the transmitted light at one wavelength versus temperature. In the first case a nearly linear shift in wavelength is observed with temperature with a sharp discontinuity at the melting point. In the second case a periodic change in intensity with temperature is recorded with a sharp deviation from periodicity at melting. Both methods lead to the same results. The experimental melting points are listed in Table 1 and are plotted in Fig. 1.

III. THEORETICAL

The thermodynamic properties of the solid and liquid phases were calculated using the methods described in detail in several of our

earlier studies of melting[10,11]. Briefly, the properties of the solid were calculated using quasi-harmonic lattice dynamics with added terms for classical and quantum anharmonic motion. The liquid properties were calculated using variational perturbation theory with a Wigner-Kirkwood quantum correction included. The intermolecular potential has been obtained in the preceding paper from a precise fit to recent high pressure shock and static data, and is expressed in the convenient exponential-six form:

$$\varphi(r) = \varepsilon\left[\frac{6}{\alpha-6}\exp[\alpha(1 - \frac{r}{r_m})] - \frac{\alpha}{\alpha-6}(\frac{r_m}{r})^6\right], \tag{1}$$

with $\alpha = 13.2$, $\varepsilon/k = 122$ K, and $r_m = 3.85 \cdot 10^{-8}$ cm.

The melting point was determined by plotting the Gibbs free energy isotherms of the liquid and solid against pressure and finding the intersection point; that is, $G(P_s,T)=G(P_l,T)$ for $P_s=P_l$ and $T_s=T_l$. The results of these calculations are plotted in Fig. 1 and listed in Table 2. The agreement between theory and experiment in Fig. 1 is very good,

limited only by the scatter in the experimental data. Although our present measurements have been restricted to determining pressures and temperatures, several earlier workers have reported melting and freezing volumes[12,13]. These are shown in Fig. 2 and compared with our predicted values. The agreement is good near the triple point, but grows worse with increasing temperature. This may be due to the failure of the simple exponential-six potential to fit the equation of state accurately at comparatively low pressures.

Because accurate calculations of the free energy have until now been difficult to make, semi-empirical models have been widely used to predict high pressure melting curves. Two of these are the Lindemann Law for melting[14] and the rule of constant packing fraction for freezing[15]. Both of these are consistent with the view that on a microscopic level the spatial configuration of the atoms at melting is invariant at all temperatures. The Lindemann Law assumes that a solid melts when the amplitude of the atomic vibrations exceed a certain fraction of the lattice spacing. This leads to the relationship

$$\frac{<R^2>}{a^2} = \frac{3kT_m(\hbar/k)^2}{M\Theta_E^2 a^2} ,$$

$$(2)$$

where T_m is the melting temperature, a is the nearest neighbor spacing, Θ_E is the Einstein temperature, and M is the atomic mass. The liquid analog of the Lindemann Law states that the liquid packing fraction,

$$\eta = \frac{\pi N d^3}{6V_m} ,$$

$$(3)$$

where d is the hard sphere diameter determined from the fluid perturbation theory, is a constant along the freezing curve. The calculated values of $<R^2>/a^2$ and η are seen in Table 2 to be nearly constant and thus these empirical relations for Ar are justified.

The invariance of the liquid order along the freezing curve is nicely demonstrated in Fig. 3 by a comparison of the pair distribution function g(r/a) calculated at the triple point (T = 83.81 K, V=28.1

cm^3/mol) and 800 K (V = 15.57 cm^3/mol) using the Monte Carlo method with the potential of Eq. 1. The results are plotted in reduced units r/a, where a = (3V/4πN)$^{1/3}$.

IV. DISCUSSION

In the preceding paper it has been suggested that solid argon might serve as a useful standard to pressures up to 3 or 4 Mbar. Pressure is routinely determined in a diamond cell by recording the shift of the R1 ruby fluorescence line which has been calibrated against isotherms reudced from shock data. But the fluorescence line broadens and accurate pressure measurements become increasingly difficult as the temperature is raised to several hundred degrees above room temperature.

In the past almost all diamond cell work has been carried out at room temperature and below, and this has not introduced any difficulties. But current advances are making it clear that in the future high temperature diamond cell research will be pursued vigorously. Thus the possibility of using argon both as a hydrostatic medium and as a pressure standard at high and low temperatures deserves some consideration. The melting curve presented in Table 2 introduces

an obvious boundary to the range of useful pressures and temperatures. For this reason it would be useful if the melting density measurements for argon could be extended to higher pressures. These would provide more data for construction of an accurate equation of state.

TABLE 1

Melting points of Ar determined from the externally heated diamond cell.

visual method		interference method	
$T_m(K)$	$P_m(kbar)$	$T_m(K)$	$P_m(kbar)$
379	24.30	474	31.96
386	24.45	531	39.00
393	25.50	626	47.69
431	26.15	622	50.00
402	27.86	652	53.50
505	32.95	658	55.40
515	35.15	668	55.92
537	35.65	717	60.35
502	35.97		

TABLE 2

Theoretical melting curve for Ar and comparison with simple models

T	P	V_s	$\Delta V/V_s$	$\Delta S/R$	η	$\sqrt{<R^2>}/a^2$
(K)	(kbar)	(cm^3/mol)				
83.81	0.094	24.86	0.136	1.718	0.455	0.096
100	0.81	24.25	0.113	1.561	0.459	0.097
200	6.75	21.25	0.071	1.241	0.465	0.101
300	14.31	19.41	0.060	1.164	0.464	0.102
400	23.36	18.07	0.054	1.120	0.464	0.103
600	44.56	16.22	0.047	1.078	0.463	0.103
800	70.03	14.92	0.044	1.054	0.463	0.103
1000	98.65	13.95	0.041	0.965	0.463	0.103
1500	183.0	12.24	0.038	0.947	0.462	0.103
2000	283.1	11.11	0.034	0.932	0.461	0.105
2500	401.5	10.23	0.032	0.920	0.461	0.105
3000	531.6	9.56	0.031	0.915	0.460	0.105

REFERENCES

1. M. Ross, H. K. Mao, P. M. Bell, and J. A. Xu, preceding paper.

2. L. W. Finger, R. M. Hazen, G. Zou, H. K. Mao, and P. M. Bell, Appl. Phys. Lett. 39, 892 (1981).

3. W. J. Nellis and A. C. Mitchell, J. Chem. Phys. 73, 6137 (1980).

4. F. V. Grigoriev, S. B. Kormer, O. L. Mikhailova, M. A. Mochalov, and V. D. Urlin, Sov. Phys. JETP 61, 751 (1985) [Zh. Eksp. Teor. Fiz. 88, 1271 (1985)].

5. D. H. Liebenberg, R. L. Mills, and J. C. Bronson, J. Appl. Phys. 45, 741 (1974).

6. P. H. Lahr and W. G. Eversole, J. Chem. Eng. Data 7, 42 (1962).

7. J. D. Grace and G. C. Kennedy, J. Phys. Chem. Solids 28, 977 (1967).

8. R. G. Crafton, Phys. Lett. 36A, 121 (1971).

9. C-S. Zha and R. Boehler, Phys. Rev. B 31, 3199 (1985).

10. D. A. Young and M. Ross, J. Chem. Phys. $\underline{74}$, 6950 (1981).

11. D. A. Young, A. K. McMahan, and M. Ross, Phys. Rev. B $\underline{24}$, 5119 (1981).

12. V. M. Cheng, W. B. Daniels, and R. K. Crawford, Phys. Lett. $\underline{43A}$, 109 (1973).

13. R. K. Crawford, in Rare Gas Solids, M. L. Klein and J. A. Venables, eds. (Academic, London, 1976) vol. II, Chap. 11.

14. S. M. Stishov, Sov. Phys. Usp. $\underline{17}$, 625 (1975) [Usp. Fiz. Nauk $\underline{114}$, 3 (1974)].

15. N. W. Ashcroft and J. Lekner, Phys. Rev. $\underline{145}$, 83 (1966).

FIGURE CAPTIONS

Fig. 1   Experimental and theoretical Ar melting curves.

Fig. 2   Experimental and theoretical melting and freezing volumes.

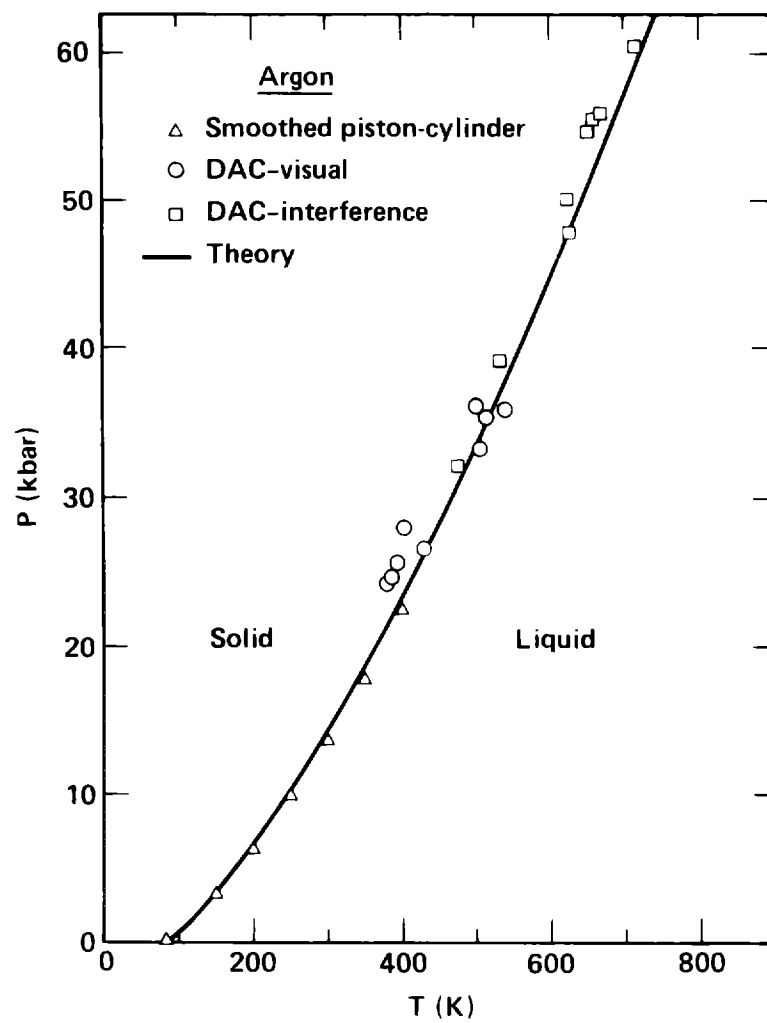Fig. 3   Monte Carlo pair distribution functions g(r/a) plotted vs. r/a, where a = $(3V/4\pi N)^{1/3}$.
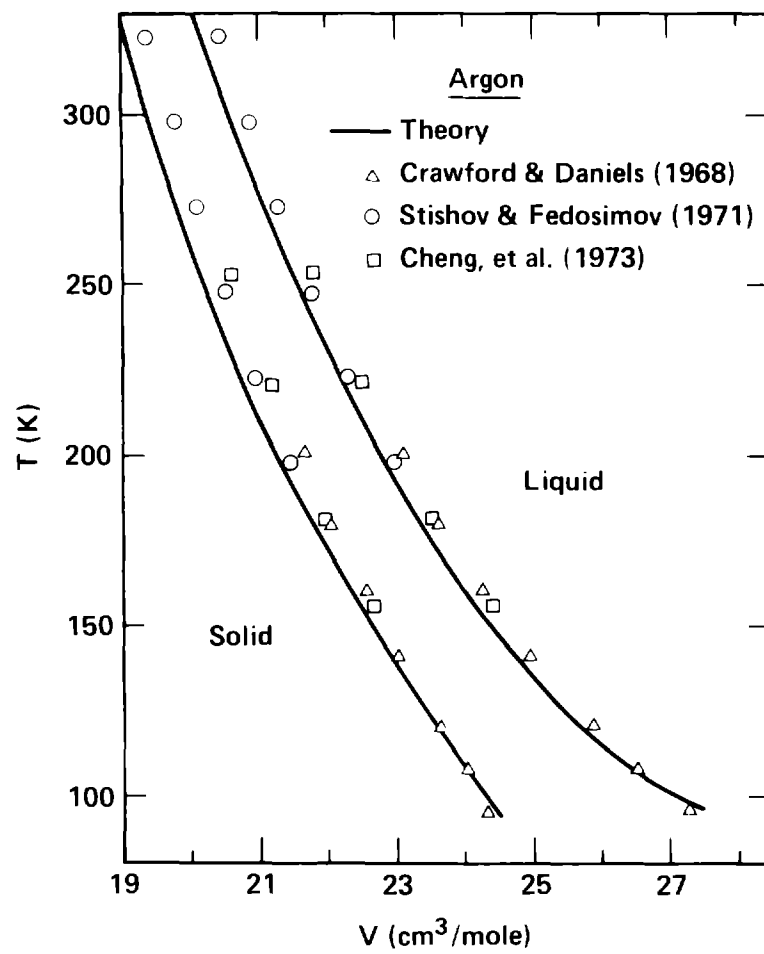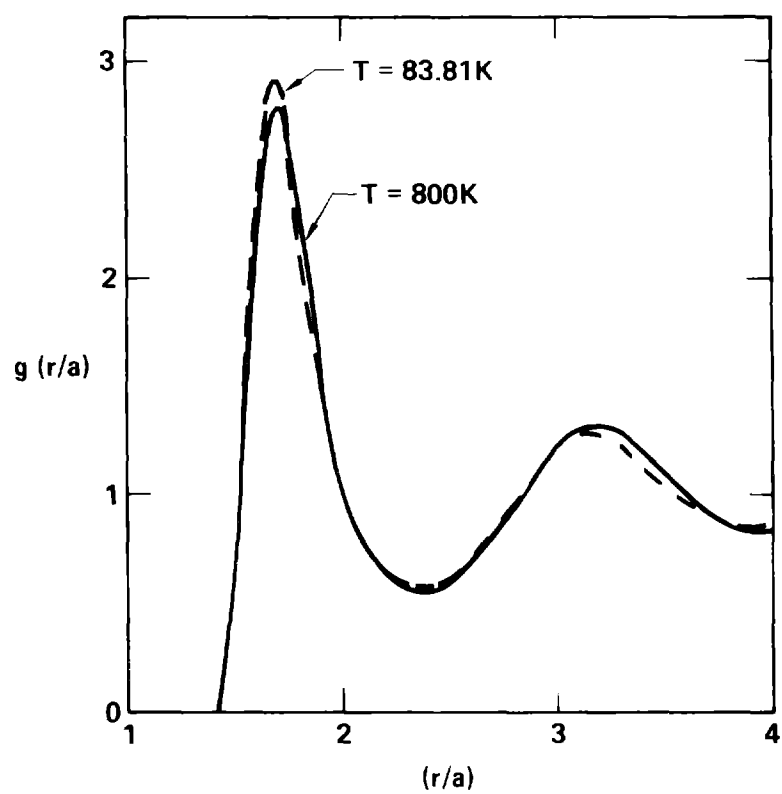
Fig. 1

Fig. 2

Fig. 3